CrossMark
click for updates

Human-Specific Bacterial Pore-Forming Toxins Induce Programmed Necrosis in Erythrocytes

Timothy J. LaRocca,[a] Elizabeth A. Stivison,[b] Eldad A. Hod,[c] Steven L. Spitalnik,[c] Peter J. Cowan,[d] Tara M. Randis,[a] Adam J. Ratner[a]

Department of Pediatrics,[a] Institute of Human Nutrition,[b] and Department of Pathology and Cell Biology,[c] Columbia University, New York, New York, USA; Immunology Research Center, St. Vincent's Hospital, Melbourne, Australia[d]

ABSTRACT   A subgroup of the cholesterol-dependent cytolysin (CDC) family of pore-forming toxins (PFTs) has an unusually narrow host range due to a requirement for binding to human CD59 (hCD59), a glycosylphosphatidylinositol (GPI)-linked complement regulatory molecule. hCD59-specific CDCs are produced by several organisms that inhabit human mucosal surfaces and can act as pathogens, including *Gardnerella vaginalis* and *Streptococcus intermedius*. The consequences and potential selective advantages of such PFT host limitation have remained unknown. Here, we demonstrate that, in addition to species restriction, PFT ligation of hCD59 triggers a previously unrecognized pathway for programmed necrosis in primary erythrocytes (red blood cells [RBCs]) from humans and transgenic mice expressing hCD59. Because they lack nuclei and mitochondria, RBCs have typically been thought to possess limited capacity to undergo programmed cell death. RBC programmed necrosis shares key molecular factors with nucleated cell necroptosis, including dependence on Fas/FasL signaling and RIP1 phosphorylation, necrosome assembly, and restriction by caspase-8. Death due to programmed necrosis in RBCs is executed by acid sphingomyelinase-dependent ceramide formation, NADPH oxidase- and iron-dependent reactive oxygen species formation, and glycolytic formation of advanced glycation end products. Bacterial PFTs that are hCD59 independent do not induce RBC programmed necrosis. RBC programmed necrosis is biochemically distinct from eryptosis, the only other known programmed cell death pathway in mature RBCs. Importantly, RBC programmed necrosis enhances the growth of PFT-producing pathogens during exposure to primary RBCs, consistent with a role for such signaling in microbial growth and pathogenesis.

IMPORTANCE   In this work, we provide the first description of a new form of programmed cell death in erythrocytes (RBCs) that occurs as a consequence of cellular attack by human-specific bacterial toxins. By defining a new RBC death pathway that shares important components with necroptosis, a programmed necrosis module that occurs in nucleated cells, these findings expand our understanding of RBC biology and RBC-pathogen interactions. In addition, our work provides a link between cholesterol-dependent cytolysin (CDC) host restriction and promotion of bacterial growth in the presence of RBCs, which may provide a selective advantage to human-associated bacterial strains that elaborate such toxins and a potential explanation for the narrowing of host range observed in this toxin family.

Address correspondence to Adam J. Ratner, ar127@columbia.edu.

Erythrocytes (red blood cells [RBCs]) are circulating, terminally differentiated cells that transport O_2 and CO_2 in all mammals, including humans. Mature human RBCs circulate for ~120 days and are cleared by several distinct mechanisms (1). Genetic, inflammatory, or immune-mediated processes (e.g., sickle cell disease, hereditary spherocytosis, and cold agglutinin disease) can shorten the RBC life span, producing anemia with serious clinical consequences (2, 3). Due to their lack of nuclei and mitochondria and their inability to synthesize proteins, mature RBCs were thought to be incapable of sophisticated cellular processes such as programmed cell death (PCD). Recently, eryptosis, a Ca^{2+}-dependent PCD unique to RBCs, was proposed to serve as an apoptosis-like process for triggering RBC clearance by macrophages (4). Thus, there is an expanding appreciation for the potential role of PCD in RBC biology and in the pathophysiology of

anemia in various settings, including heart failure, sickle cell disease, and malaria (4).

Pore-forming toxins (PFTs) are bacterial virulence factors that bind host cell receptors, oligomerize, and insert a functional pore into the membrane that may induce osmotic lysis (5). Pore formation triggers target cell signaling pathways, including proinflammatory, membrane repair, and PCD modules (5). The cholesterol-dependent cytolysins (CDCs) constitute a PFT subfamily that relies on cholesterol binding (6). Most CDC monomers bind directly to cholesterol, but a subset requires ligation of human CD59 (hCD59), a glycosylphosphatidylinositol (GPI)-anchored complement regulatory molecule, thereby restricting their host range (6–8). PFTs induce RBC death and are thus termed hemolytic; however, this hemolytic ability is often used solely as a measure of the functionality of these toxins in the lab-

oratory. The progression and role of RBC death in response to attack by bacterial PFTs and its relevance to host-pathogen interactions have been underappreciated. Many PFT-producing pathogens may come into contact with RBCs in the course of colonization or disease, including *Gardnerella vaginalis*, *Streptococcus intermedius*, and *Streptococcus pneumoniae* (9–11). Some of these pathogens can enter the RBC-dominated bloodstream, causing bacteremia, aiding in dissemination and pathogenesis (9, 10, 12, 13). In some cases, bacteremic infections can also lead to acquired (hemolytic) anemia (3). Additionally, *G. vaginalis*, associated with bacterial vaginosis, proliferates and colonizes to its highest levels at the vaginal mucosa during menses (11). Thus, the interaction of PFT-producing pathogens with mature RBCs has relevance to mechanisms of colonization and disease.

Here, we show that vaginolysin (VLY) and intermedilysin (ILY), hCD59-specific PFTs produced by *G. vaginalis* and *S. intermedius*, respectively, induce programmed necrosis (necroptosis) in mature RBCs. Similarly to programmed necrosis in nucleated cells (14), RBC programmed necrosis depends on Fas receptor and Fas ligand (Fas/FasL), RIP1 kinase phosphorylation, and mixed-lineage kinase domain-like (MLKL) protein. RBC programmed necrosis is also associated with assembly of a cytosolic complex called the necrosome (14). Also similarly to programmed necrosis in nucleated cells (14), this PCD is antagonized by caspase-8 in mature RBCs. Downstream effector pathways involved in the execution of RBC programmed necrosis included the formation of ceramide by acid sphingomyelinase (aSMase), formation of reactive oxygen species (ROS) by NADPH oxidase (NOX) and iron in the Fenton reaction, and formation of advanced glycation end products (AGEs) via glycolysis. Importantly, we show that RBC programmed necrosis is distinct from eryptosis, the only other known form of PCD in RBCs. Finally, the induction of RBC programmed necrosis enhances the growth of PFT-producing bacteria, suggesting a role for this PCD in the pathogenesis of these organisms.

RESULTS

VLY, an hCD59-specific PFT, causes lipid raft enlargement and recruitment of PCD factors to lipid rafts of mature RBCs. While analyzing the interaction of VLY with lipid rafts of mature primary human RBCs, we observed an increase in lipid raft-associated proteins (hCD59 and flotillin-1) and lipids (cholesterol, GM1, and GT1b) in detergent-resistant membrane (DRM) fractions derived from lipid rafts (Fig. 1A and B). This indicates an increase in the size/stability of lipid rafts, which occurs during lipid raft-dependent signaling (15, 16). Fas receptor (Fas) and Fas ligand (FasL), which induce extrinsic PCD (17), were also recruited to DRM fractions upon VLY treatment (Fig. 1C). Fas and FasL exist outside lipid rafts in resting cells (18), and their recruitment to these signaling microdomains, in addition to an increase in raft size, suggested activation of PCD in mature RBCs. The cytosolic protein hemoglobin (HGB) did not differ in localization upon VLY stimulation.

hCD59-dependent PFTs induce Fas/FasL-dependent death of mature human and transgenic murine RBCs. Because Fas and FasL were recruited to lipid rafts in human RBCs following attack by VLY, we hypothesized that this hCD59-specific PFT and other bacterial PFTs might cause Fas/FasL-dependent death of mature RBCs. Thus, we analyzed the hemolytic activity of several purified, recombinant PFTs (see Fig. S1 in the supplemental material) at
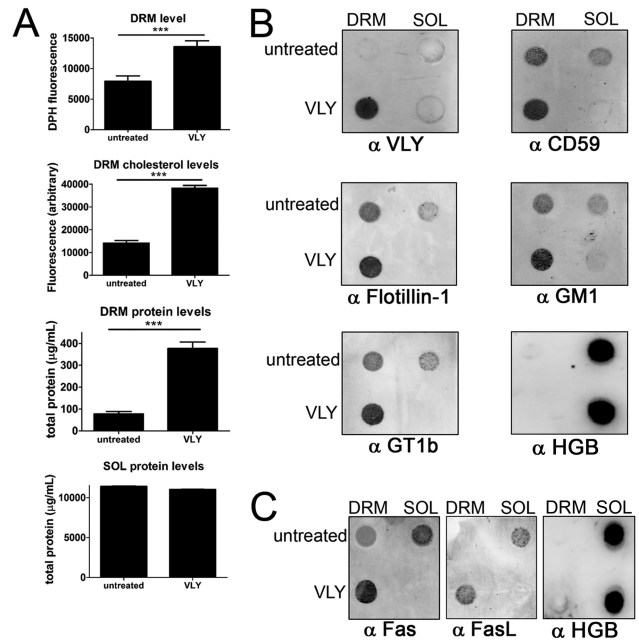

FIG 1 VLY, an hCD59-specific PFT, induces lipid raft enlargement, including recruitment of Fas and FasL. (A) RBC detergent-resistant membranes (DRMs) increase in abundance in response to VLY as measured by DPH fluorescence. Cholesterol and proteins increase in DRMs after VLY treatment, with most proteins remaining soluble (SOL). (B) Dot blots showing that raft-associated proteins (CD59 and flotillin-1) and lipids (GM1 and GT1b) increase in DRMs in response to VLY. Hemoglobin (HGB) is excluded from DRMs. (C) Fas and FasL, normally excluded from rafts, are recruited to DRMs in response to VLY. ***, $P < 0.001$ (Student's t test).

different hemolytic doses, with 1 hemolytic unit (HU) corresponding to 50% hemolysis (see Fig. S2). Indeed, VLY and ILY, which are hCD59-specific PFTs, caused RBC death that was inhibited by monoclonal antibody (MAb) neutralization of FasL (Fig. 2A and B). The hCD59-independent PFTs pneumolysin (PLY; from *Streptococcus pneumoniae*) and alpha-toxin (A-tox; from *Staphylococcus aureus*) did not cause FasL-dependent RBC death (Fig. 2B). VLY, ILY, and PLY are CDCs that may form pores with an external diameter of >15 nm, whereas A-tox is not a CDC and forms pores of 1 to 2 nm in diameter (5, 6). Exogenous recombinant FasL (rFasL) significantly enhanced VLY-mediated RBC death (Fig. 2C), as did an agonistic MAb targeting Fas (Fig. 2D). Notably, low hemolytic doses of all PFTs tested were enhanced when combined with rFasL or agonistic Fas MAb (Fig. 2E and F). We used hCD59 transgenic murine RBCs as a model system, as these are susceptible to VLY and ILY, whereas nontransgenic cells are resistant (Fig. 2G and H). Death of hCD59-transgenic murine RBCs induced by VLY or ILY, but not PLY, was inhibited by FasL neutralization, indicating that FasL-dependent death can be initiated in nonhuman RBCs (Fig. 2H). These results indicate that hCD59-specific PFTs initiate Fas/FasL signaling in RBCs resulting in death and that the combination of Fas/FasL signaling and pore formation primes RBCs for death by any PFT.

hCD59-specific bacterial PFTs induce RIP1-dependent programmed necrosis in mature RBCs. Because hCD59-specific PFTs caused Fas/FasL-dependent RBC death, we hypothesized
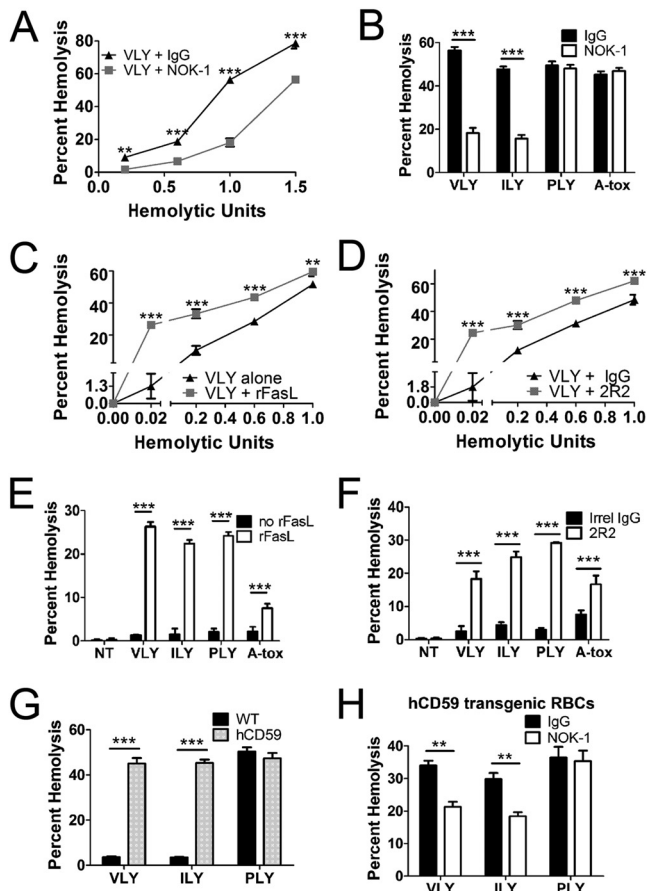
FIG 2 VLY and ILY, hCD59-specific PFTs, induce Fas/FasL-dependent death in human and hCD59-transgenic murine RBCs. (A) Neutralization of FasL with a MAb (NOK-1, 1 μg/ml) inhibits RBC death by VLY. (B) NOK-1 inhibits RBC death by VLY or ILY but not by hCD59-independent PLY or A-tox. (C and D) Exogenous rFasL (0.1 μg/ml) (C) or agonistic Fas MAb (2R2, 1 μg/ml) (D) enhances RBC death by VLY. (E and F) rFasL (E) or 2R2 (F) enhances RBC death caused by all PFTs tested. (G) C57BL/6J (nontransgenic) RBCs are resistant to VLY and ILY but sensitive to PLY. (H) Death of hCD59-transgenic murine RBCs by VLY or ILY is inhibited by NOK-1. IgG, irrelevant IgG. ***, *P* < 0.001; **, *P* < 0.01 (two-way analysis of variance, Bonferroni posttest).

FIG 3 VLY and ILY cause RIP1- and MLKL-dependent programmed necrosis in mature RBCs. (A) Dot blots showing recruitment of RIP1 and FADD to DRMs in response to VLY. Hemoglobin (HGB) remains in the soluble fraction (SOL). (B) Inhibition of RIP1 with nec-1 reduces RBC death by VLY relative to vehicle control. (C) Inhibition of MLKL with NSA reduces RBC death by VLY relative to vehicle control. (D to I) Inhibition of RIP1 (D) or MLKL (E) reduces RBC death by ILY and has no effect on death by PLY (F and G) or A-tox (H and I). (J) Enhanced RBC death caused by the combination of PFTs and rFasL is inhibited by nec-1 relative to vehicle control. ***, *P* < 0.001 (two-way analysis of variance, Bonferroni posttest).

that these PFTs might activate PCD in RBCs. In addition, two components of complexes formed during programmed necrosis (necroptosis) were recruited to RBC lipid rafts in response to VLY. These components, Fas-associated death domain (FADD) and RIP1 kinase (RIP1) are cytosolic and not normally associated with lipid rafts but were found in DRMs following RBC stimulation with VLY (Fig. 3A). This suggested that VLY might activate programmed necrosis, a PCD pathway that occurs in nucleated cell types and can involve induction by Fas/FasL, in mature RBCs (14, 19).

We used necrostatin-1 (nec-1), a small-molecule inhibitor of RIP1 kinase, to explore the induction of Fas/FasL-dependent programmed necrosis in mature RBCs (20). RIP1 phosphorylation and recruitment to the cytosolic necrosome complex are critical for the induction of programmed necrosis (19–21). The importance of RIP1 is such that programmed necrosis is also referred to as RIP1-dependent cell death (14). nec-1 inhibited VLY-induced RBC death over a range of concentrations (Fig. 3B). RIP3 kinase also plays important roles in programmed necrosis (22, 23) by
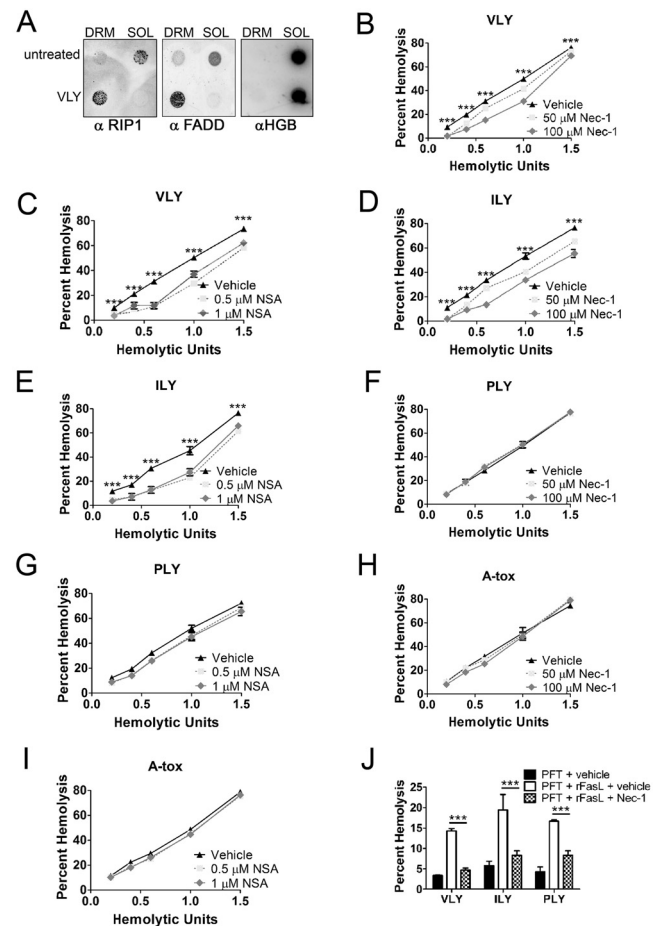
interacting with a downstream protein, mixed-lineage kinase domain-like (MLKL), to exert its effects (24). Inhibition of MLKL with necrosulfonamide (NSA) also reduced RBC death caused by VLY, consistent with a role for programmed necrosis in RBCs (Fig. 3C). Similarly, nec-1 and NSA inhibited RBC death by hCD59-dependent ILY but had no effect on hemolysis by hCD59-independent PLY and A-tox (Fig. 3D to I). These results indicated that hCD59-specific bacterial PFTs, but not hCD59-independent PFTs, induce programmed necrosis in mature RBCs. In addition, rFasL enhanced the hemolysis by all PFTs tested, regardless of intrinsic hCD59 specificity (Fig. 2E). This enhanced death was nec-1 inhibitable, indicating that the combination of Fas/FasL signaling and PFT activity initiates RIP1-dependent programmed necrosis in mature RBCs (Fig. 3J).

hCD59-specific bacterial PFTs induce FasL-dependent RIP1 phosphorylation and necrosome assembly in mature RBCs. To further explore the molecular events associated with programmed
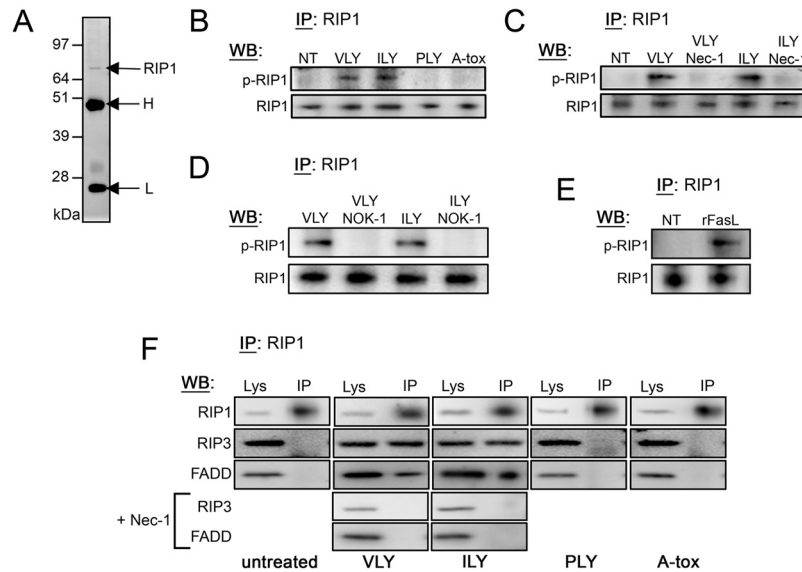
FIG 4 VLY and ILY induce FasL-dependent phosphorylation of RIP1 and necrosome assembly in RBCs. (A) Coomassie blue-stained SDS-PAGE gel showing RIP1 IP. H, IgG heavy chain; L, IgG light chain. (B to F) Immunoblots from RIP1 IPs showing RIP1 phosphorylation (p-RIP1) in response to VLY or ILY (B), prevention of p-RIP1 with nec-1 (C), prevention of p-RIP1 with NOK-1 (D), p-RIP1 induced by rFasL (E), and coprecipitation of RIP3 and FADD with RIP1 in response to VLY or ILY that is prevented by RIP1 inhibition (F). NT, no treatment.

necrosis in RBCs, RIP1 was isolated from RBCs by immunoprecipitation (IP) (Fig. 4A) and probed on immunoblots to determine its phosphorylation state in response to PFTs. RIP1 became phosphorylated (p-RIP1) in RBCs in response to VLY or ILY but not in response to hCD59-independent PFTs (Fig. 4B). RIP1 phosphorylation induced by VLY and ILY was also inhibited by nec-1, confirming the activity of this inhibitor in primary human RBCs (Fig. 4C). The induced p-RIP1 was prevented by FasL neutralization, suggesting that hCD59-specific PFTs induce p-RIP1 through downstream activity of Fas/FasL (Fig. 4D). This seems likely, as addition of rFasL alone to RBCs also resulted induced RIP1 phosphorylation (Fig. 4E). We confirmed the specificity of the IPs for RIP1, as an irrelevant IgG did not precipitate RIP1 (see Fig. S3A in the supplemental material).

Formation of the necrosome is generally associated with programmed necrosis in nucleated cells (25). Necrosomes contain important signaling proteins, RIP1, RIP3, FADD, and caspase-8 (14). To investigate necrosome assembly in RBCs, RIP1 IPs were probed for specific coprecipitants. Necrosome components RIP3 and FADD coprecipitated with RIP1 following stimulation with VLY or ILY, suggesting necrosome assembly. These associations were inhibited by nec-1 (Fig. 4F). hCD59-independent PFTs (PLY and A-tox) did not induce necrosome assembly in RBCs (Fig. 4F).

Necrosome-associated caspase-8 antagonizes RBC programmed necrosis. In nucleated cells, caspase-8 is a necrosome component that antagonizes programmed necrosis by cleaving RIP1 and RIP3 (14, 26). To determine if caspase-8 served a similar role in RBCs, we analyzed caspase-8 by IP (Fig. 5A) and found that RIP1 coprecipitated with caspase-8 in RBCs regardless of PFT stimulation, suggesting a constitutive association of these proteins in RBCs but not THP-1 cells (Fig. 5B). FADD coprecipitated with caspase-8 only in response to VLY or ILY, suggesting formation of a RIP1/FADD/caspase-8 complex in response to hCD59-specific

PFTs (Fig. 5B). Pan-caspase inhibition enhanced RBC death by VLY or ILY (Fig. 5C and D), and this enhanced death was prevented by RIP1 inhibition (Fig. 5E). Specific inhibition of caspase-8, but not caspase-3, enhanced RBC death by VLY or ILY (Fig. 5F), consistent with an antagonistic role for caspase-8 in RBC programmed necrosis similar to its function in programmed necrosis of nucleated cells (14). In agreement with this finding, caspase-8 inhibition led to an increase in RIP1 phosphorylation following VLY stimulation (Fig. 5G). The IPs were specific for caspase-8, as an irrelevant IgG did not pull down caspase-8 (see Fig. S3B in the supplemental material).

NOX/iron-dependent ROS formation and aSMase-dependent ceramide formation are downstream components of RBC programmed necrosis. Cell death by programmed necrosis may involve several different downstream effector pathways, including ceramide formation, ROS formation, phospholipase/calpain activity, and AGE formation by enhanced glycolysis (14). Effector pathways vary by cell type, and several mechanisms may be active within single cell types (14). RBC death induced by VLY and ILY was blunted by inhibition of NOX (Fig. 6A and B), and both VLY and ILY caused an increase in ROS in RBCs (Fig. 6C). Additionally, iron chelation reduced RBC death caused by VLY and ILY and prevented ROS induction by these PFTs (Fig. 6D to F). These results suggest that NOX-dependent ROS contribute to RBC death by programmed necrosis and that ROS formation is enhanced by iron, likely due to the Fenton reaction.

Inhibition of aSMase, which produces ceramide from sphingomyelin, reduced RBC death by VLY and ILY, as did MAb neutralization of ceramide (Fig. 6G to I). VLY and ILY caused significant increases in surface ceramide, whereas hCD59-independent PFTs did not (Fig. 6J). Thus, aSMase-dependent ceramide formation is an additional downstream component in RBC programmed necrosis.
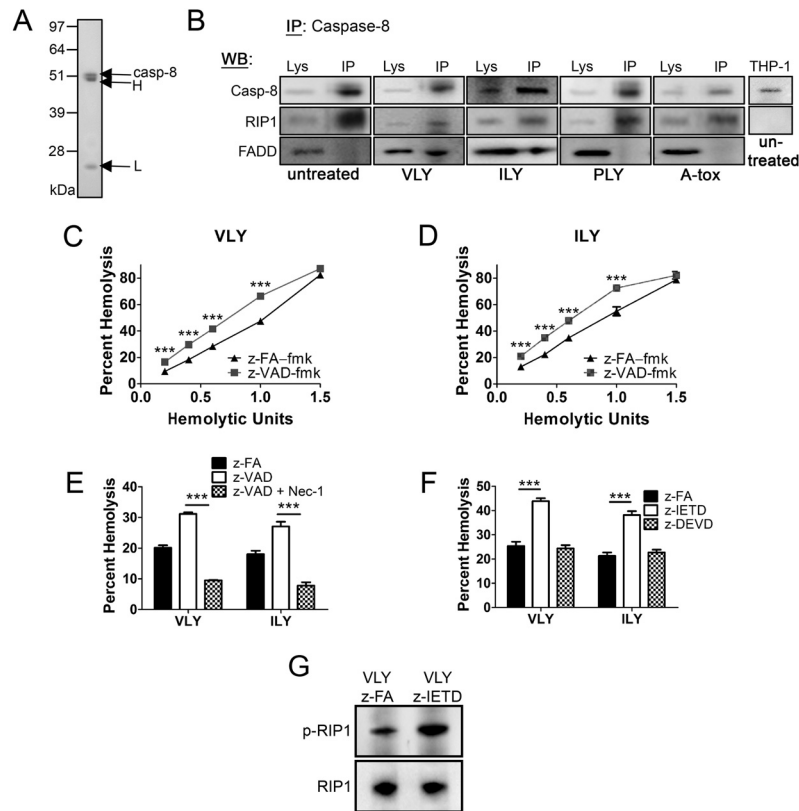
FIG 5 Caspase-8 is a necrosome component that antagonizes RBC programmed necrosis. (A) Coomassie blue-stained SDS-PAGE gel showing caspase-8 IP. H, IgG heavy chain; L, IgG light chain. (B) Immunoblots from caspase-8 IPs showing coprecipitation of RIP1 under all conditions and coprecipitation of FADD in response to VLY or ILY. RIP1 does not coprecipitate with caspase-8 in THP-1 cells. (C to E) Pan-caspase inhibition with 10 μM z-VAD-fmk enhanced RBC death by VLY or ILY (C and D, respectively) and was prevented by nec-1 (E). (F) Specific inhibition of caspase-8 with 10 μM z-IETD-fmk enhanced RBC death caused by VLY or ILY. Caspase-3 inhibition (10 μM z-DEVD-fmk) had no effect. (G) Levels of p-RIP1 increase in RBCs following inhibition of caspase-8 (z-IETD) relative to a caspase inhibitor negative control (z-FA). ***, $P < 0.001$ (two-way analysis of variance, Bonferroni posttest). z-FA-fmk, caspase inhibitor negative control.

Glycolytic formation of AGEs contributes to the execution of RBC programmed necrosis. AGE formation may occur downstream of programmed necrosis in nucleated cells due to increased glycolysis (27). Exogenous glucose enhanced RBC death by VLY and ILY in a RIP1-dependent manner (Fig. 7A). Glycolysis drove this process, as a nonmetabolizable glucose analog, 2-deoxy-D-glucose, did not affect PFT-mediated RBC death (Fig. 7B). Importantly, glucose uptake had no effect on RBC death by the hCD59-independent PFT, PLY (Fig. 7C). That glycolysis participates in RBC programmed necrosis suggests the involvement of AGEs (27). Indeed, specific inhibition of AGEs reduced RBC death by VLY and ILY (Fig. 7D and E) and prevented enhancement of RBC death by glucose uptake (Fig. 7F). Using a whole-cell fluorescence assay, we detected an increase in AGE formation in response to VLY and ILY but not PLY (Fig. 7G). These results show that glycolytic AGE formation plays a crucial role in the demise of RBCs by programmed necrosis.

RBC programmed necrosis is distinct from eryptosis. Although the identification of programmed necrosis in RBCs in response to hCD59-specific PFTs was unexpected, there is a precedent in eryptosis, a PCD unique to RBCs, which was recently described (4). To determine if RBC programmed necrosis was distinct from eryptosis, two well-characterized eryptotic stimuli, hyperosmotic stress and excess calcium, were used (28, 29). Hy-

perosmotic or calcium-induced eryptosis was not affected by nec-1, did not induce p-RIP1, did not depend on FasL, and was not enhanced by rFasL addition (Fig. 8A to D). Moreover, factors on which eryptosis depends (e.g., intracellular Ca^{2+} and p38 mitogen-activated protein kinase [MAPK] [4, 30]) played no role in RBC programmed necrosis induced by hCD59-specific PFTs (Fig. 8E and F). Thus, programmed necrosis is a new PCD pathway in mature RBCs that is distinct from eryptosis.

Induction of RBC programmed necrosis enhances bacterial growth *in vitro*. hCD59-specific PFTs induce Fas/FasL-dependent programmed necrosis of mature RBCs while hCD59-independent PFTs do not. This observation raises the question of the potential benefit that RBC programmed necrosis may have for PFT-producing pathogenic bacteria. We hypothesized that induction of programmed necrosis might increase RBC killing at low organism or PFT concentrations, resulting in more efficient release of nutrients that might enhance bacterial growth. To this end, a series of bacterial growth assays were performed during which *G. vaginalis*, *S. intermedius*, and *S. pneumoniae* were cultured with or without human RBCs. Using RIP1 IP and immunoblotting, we confirmed that live *G. vaginalis* and *S. intermedius* induced p-RIP1 (Fig. 9A and B). RIP1 phosphorylation was induced by native VLY or ILY, respectively, as it was prevented by an anti-CDC antibody (31) (Fig. 9A and B; see also Fig. S4 in the
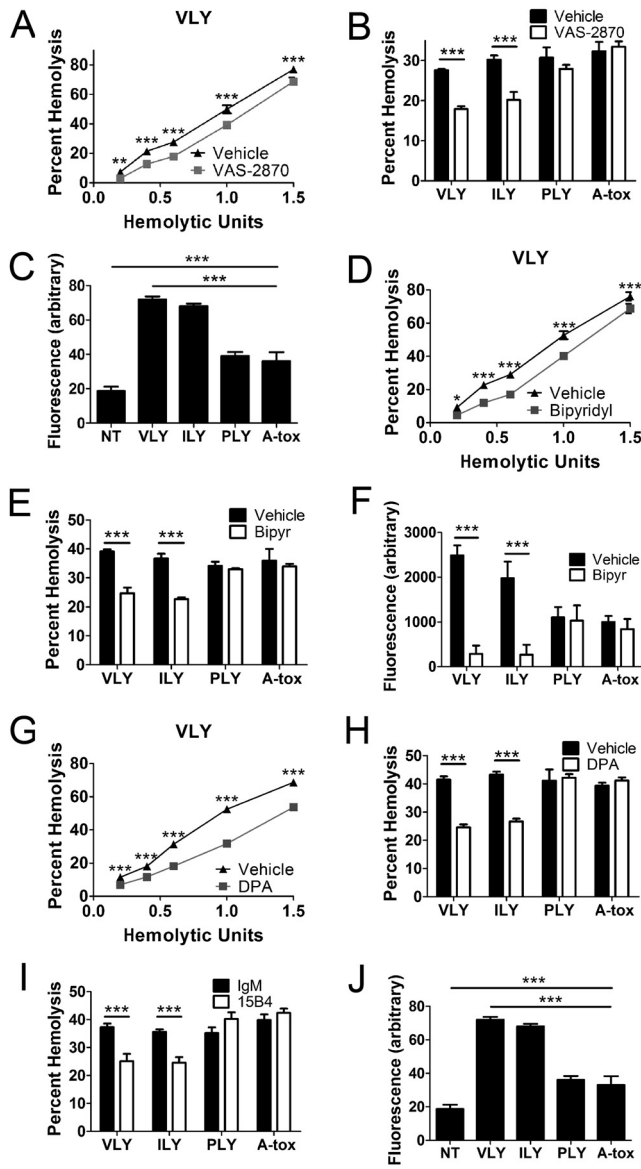
FIG 6 RBC programmed necrosis is executed in part by aSMase-dependent ceramide formation and NOX/iron-dependent ROS. (A and B) NOX inhibition with 10 μM VAS-2870 reduces RBC death by VLY and ILY compared to vehicle control. (C) VLY and ILY induce ROS in RBCs as measured by DCFDA. (D and E) Iron chelation with 100 μM 2,2-bipyridyl reduces RBC death by VLY or ILY relative to vehicle control. (F) Iron chelation prevents ROS induction by VLY and ILY. (G and H) Inhibition of aSMase with 20 μM desipramine (DPA) reduced RBC death by VLY and ILY relative to vehicle control. (I) Ceramide neutralization with MAb 15B4 reduced death by VLY or ILY relative to irrelevant IgM (IgM). (J) VLY and ILY induce surface ceramide as determined by immunofluorescence. ***, $P < 0.001$ (two-way analysis of variance, Bonferroni posttest).
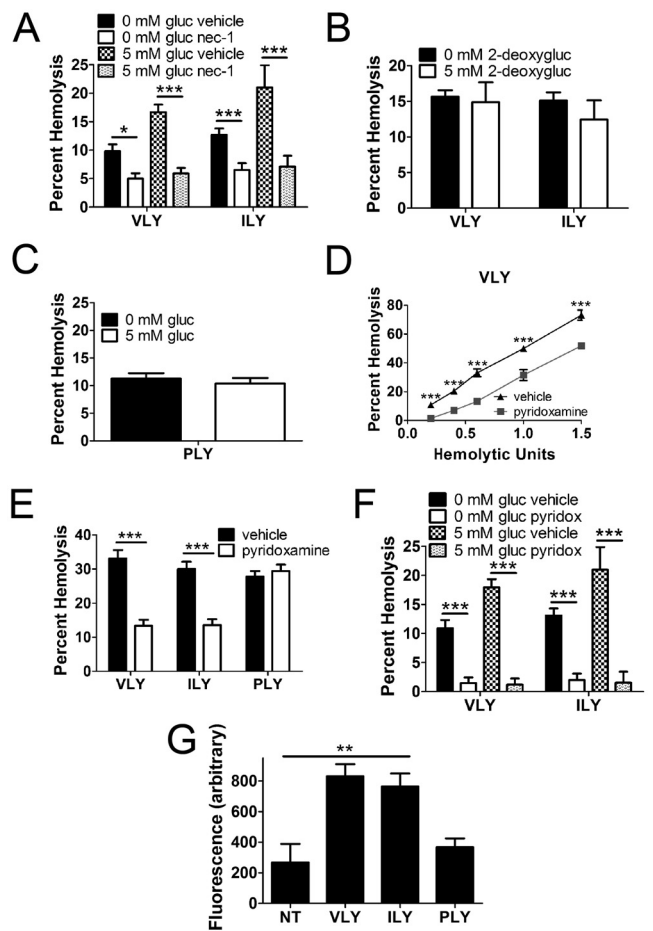
FIG 7 Glycolytic formation of AGEs is a component in the execution of RBC programmed necrosis. (A) Glucose (gluc) uptake by RBCs in a 5 mM solution enhanced death by VLY or ILY and was prevented by nec-1. (B) Uptake of the nonmetabolizable 2-deoxy-D-glucose (2-deoxygluc) had no effect on RBC death. (C) Glucose uptake had no effect on RBC death by the hCD59-independent PLY. (D and E) AGE inhibition with 1 mM pyridoxamine reduced death by VLY or ILY relative to vehicle control. (F) RBC death enhanced by glucose uptake is prevented by AGE inhibition. (G) VLY and ILY induce RBC AGE formation as determined by whole-cell immunofluorescence assay. ***, $P < 0.001$; **, $P < 0.01$; *, $P < 0.05$ (two-way analysis of variance, Bonferroni posttest).

supplemental material). *G. vaginalis* growth required RBCs, whereas *S. intermedius* growth was significantly enhanced in the presence of RBCs (Fig. 9C and D). Neutralization of RBC FasL reduced *G. vaginalis* and *S. intermedius* growth in the presence of human RBCs (Fig. 9C and D), suggesting that FasL-dependent programmed necrosis of RBCs enhanced the proliferation of *G. vaginalis* and *S. intermedius*. Consistent with the finding that the hCD59-independent PLY did not induce FasL-dependent

RBC programmed necrosis, the growth of *S. pneumoniae* (which produces PLY) was unaffected by FasL neutralization in RBCs (Fig. 9E).

Addition of exogenous rFasL allowed all bacterial PFTs to cause RBC programmed necrosis, resulting in enhanced RBC death, regardless of intrinsic hCD59 specificity (Fig. 2E and 3J). Consistent with this observation, addition of rFasL to human RBCs enhanced bacterial growth by hCD59-specific PFT-producing *G. vaginalis* and *S. intermedius* as well as by hCD59-independent PFT-producing *S. pneumoniae* (Fig. 9F to H). Collectively, these results demonstrate that the induction of RBC programmed necrosis enhances bacterial growth. Consistent with the hypothesis that release of RBC cytosolic contents might provide nutrients to prime bacterial growth, addition of purified hemoglobin to cultures also enhanced the growth of all three species tested (see Fig. S5 in the supplemental material).
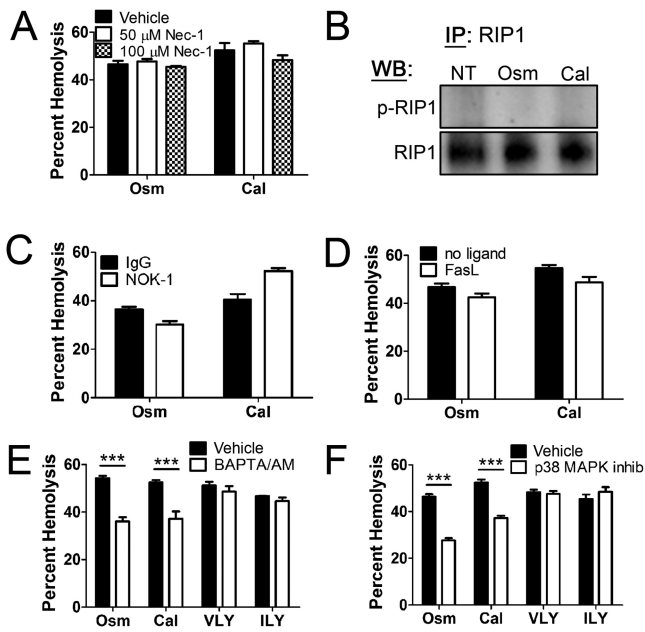
FIG 8 RBC programmed necrosis differs from eryptosis. (A) Eryptosis by hyperosmotic stress (Osm) or excess calcium (Cal) is not inhibited by nec-1. (B) RIP1 IPs showing that eryptosis does not induce p-RIP1. (C and D) Eryptosis is unaffected by NOK-1 (C) or rFasL (D). (E and F) Eryptosis depends on intracellular Ca^{2+} as shown by chelation with 10 μM BAPTA/AM [1,2-bis(o-aminophenoxy)ethane-N,N,N',N'-tetraacetic acid–acetoxymethyl ester] (E) and p38 mitogen-activated protein kinase (MAPK) as shown by inhibition with 10 μM p38 MAPK inhibitor III (Calbiochem) (F) while RBC programmed necrosis by VLY or ILY does not. ***, $P < 0.001$ (two-way analysis of variance, Bonferroni posttest).

DISCUSSION

RBC programmed necrosis: a new form of PCD induced by bacterial PFTs. These findings provide evidence for the induction of a previously unidentified PCD pathway in mature RBCs by human-specific bacterial PFTs. RBC programmed necrosis was activated by hCD59-specific CDCs VLY and ILY but not by other PFTs. RBC programmed necrosis depended on Fas/FasL, RIP1 phosphorylation, and MLKL and was antagonized by caspase-8. RBC programmed necrosis was also associated with necrosome assembly and was executed by aSMase-dependent ceramide formation, NOX/iron-dependent ROS production, and glycolytic AGE formation.

hCD59-independent PFTs (i.e., PLY and A-tox) did not activate RBC programmed necrosis, consistent with an important role for hCD59 binding/signaling. However, these PFTs did activate RBC programmed necrosis when combined with exogenous rFasL or a Fas-specific agonistic MAb. That hCD59-independent PFTs can produce RBC programmed necrosis in combination with rFasL is significant, because many infections *in vivo* have high levels of circulating FasL (32, 33). Similarly, as members of the tumor necrosis factor (TNF) superfamily, there are infectious settings in which high levels of other known necroptotic stimuli (e.g., TNF-α and TRAIL) are seen (34). Induction of RBC programmed necrosis by rFasL combined with PFT suggests that FasL functions downstream of hCD59 binding/signaling by VLY or ILY. This is supported by the finding that FasL neutralization prevents RIP1 phosphorylation by VLY or ILY and that rFasL alone induces RIP1 phosphorylation in RBCs.

RBC programmed necrosis and eryptosis are distinct. The discovery of programmed necrosis in RBCs by hCD59-specific PFTs is not the first instance of RBC PCD. Eryptosis is a Ca^{2+}-, p38 MAPK-dependent PCD process in RBCs (4). It is characterized by phosphatidylserine externalization and ceramide formation, marking these RBCs for macrophage ingestion (4, 18). Our results demonstrate that RBC programmed necrosis differs from eryptosis, functioning as an independent, previously unrecognized PCD pathway in mature RBCs. It is possible that eryptosis contributes to "natural" RBC death/removal due to noninfectious injury, whereas programmed necrosis is induced by infection with PFT-producing pathogens.

Significance of RBC programmed necrosis. hCD59-specific PFT induction of RBC programmed necrosis is significant for at least two reasons: (i) it provides new understanding of the relevance of programmed necrosis to RBC biology and physiology and (ii) it suggests that RBC programmed necrosis may play a role in colonization or pathogenesis of hCD59-specific PFT-producing pathogens. Whereas eryptosis is important, it does not share key molecular features of PCD that occur in nucleated cells, including caspase dependence (whereas senescent and storage-damaged RBCs display active caspases [35, 36], these critical apoptotic enzymes have not been conclusively linked to eryptosis [28, 37, 38]) and the requirement of extrinsic ligands of the TNF superfamily (37). Therefore, eryptosis is a PCD unique to mature RBCs that is not shared with nucleated cells. Conversely, RBC programmed necrosis proceeds in a manner molecularly similar to nucleated cell necroptosis, sharing many key features. These include dependence on RIP1 phosphorylation, MLKL, and extrinsic ligands of the TNF superfamily (e.g., FasL); antagonism by caspase-8; and necrosome assembly. Moreover, whereas Fas and FasL differ in their cellular localizations during oxidative stress and in senescent RBCs (18), they were reported to be nonfunctional in mature RBCs (37, 39). Nonetheless, we show that Fas and FasL drive programmed necrosis in mature RBCs, promoting RIP1 phosphorylation. The intimate involvement of Fas/FasL in RBC programmed necrosis may explain the differential localization of Fas/FasL previously seen in senescent RBCs (18), suggesting that aged RBCs may be primed for programmed necrosis. These findings expand our knowledge of RBC physiology by identifying other PCD pathways in RBCs. Given the similarities of programmed necrosis in RBCs and nucleated cells, we speculate that caspase-dependent apoptosis, resembling that of nucleated cells, may occur in mature RBCs. Alternatively, it is possible that mature RBCs have lost the capacity for classical apoptosis but retained the capacity for programmed necrosis.

As RBC programmed necrosis enhanced bacterial proliferation *in vitro*, this PCD may play a role in bacterial growth and pathogenesis *in vivo*. *G. vaginalis* colonizes the lower genital tract of women (11). The growth/presence of *G. vaginalis* varies throughout the menstrual cycle, with the highest levels of *G. vaginalis* occurring during menses (11). This suggests that RBC availability may affect bacterial growth. We speculate that VLY-mediated RBC programmed necrosis plays a significant role in the pathogenesis of bacterial vaginosis. In addition, *S. intermedius* infection is associated with abscess formation in the brain and liver, resulting from hematogenous spread from mucosal surfaces (10). As RBC programmed necrosis enhances *S. intermedius* growth *in vitro*, we speculate that this PCD may aid its dissemination and growth. The potential for increased bacterial growth during the
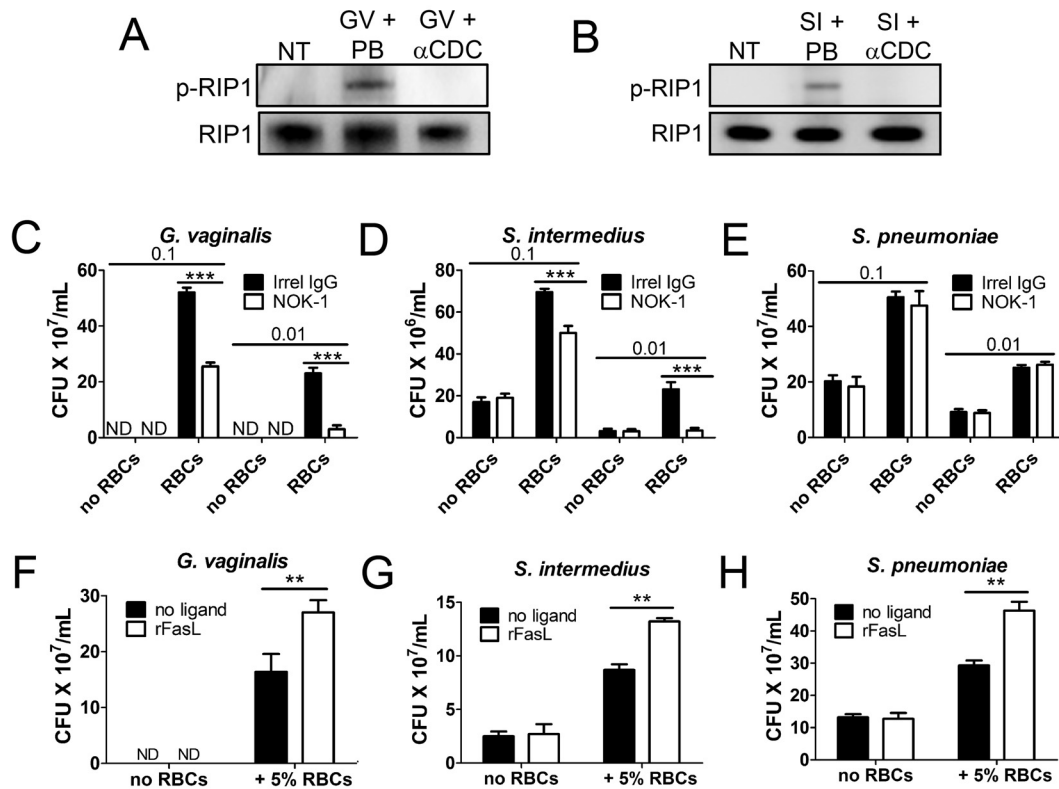
FIG 9 RBC programmed necrosis enhances growth of PFT-producing pathogenic bacteria *in vitro*. (A and B) RIP1 IPs showing p-RIP1 in response to live *G. vaginalis* (GV) or *S. intermedius* (SI). A neutralizing PAb against CDCs (αCDC) prevents p-RIP1 formation relative to control prebleed (PB) serum. (C and D) Enhanced growth of 2 starting inocula (OD_{600} of 0.1 and OD_{600} of 0.01) of *G. vaginalis* (C) or *S. intermedius* (D) in the presence of human RBCs is partially inhibited by FasL neutralization with NOK-1 relative to irrelevant IgG. (E) Growth of *S. pneumoniae*, which produces the hCD59-independent PLY, is not affected by FasL neutralization. (F to H) Addition of rFasL to cultures including human RBCs and *G. vaginalis* (F), *S. intermedius* (G), or *S. pneumoniae* (H), inoculated at an OD_{600} of 0.1, enhanced the growth of all bacteria tested. ***, $P < 0.001$; **, $P < 0.01$ (two-way analysis of variance, Bonferroni posttest).

hematogenous phase of *S. intermedius* infections as a result of RBC programmed necrosis could lead to exacerbated abscess formation due to greater bacterial burden. When considering this growth benefit, the direct induction of hCD59-specific RBC programmed necrosis by VLY and ILY might explain a potential selective advantage associated with human-specific PFT production by *G. vaginalis* and *S. intermedius*.

Pneumonia due to *S. pneumoniae* may progress to bacteremia (9), but as PLY cannot induce RBC programmed necrosis, a role for this PCD in pneumococcal infection is unclear. Nonetheless, pneumococcal infection is associated with FasL release, because *S. pneumoniae* elicits increased FasL levels in lung (40) and causes FasL-dependent bystander death following phagocytosis (41). As shown here, PLY can induce RBC programmed necrosis when combined with rFasL, raising the possibility that this PCD plays a role in systemic pneumococcal infection. These potential roles of RBC programmed necrosis in promoting the pathogenesis of different microbes are intriguing and suggest the possibility for therapeutic intervention by targeting factors specific to this PCD.

MATERIALS AND METHODS

Human cells. Primary human RBCs, with or without leukoreduction using Purecell Neo leukocyte reduction filters (Haemonetics), were obtained from healthy volunteers under a protocol approved by the Columbia University Institutional Review Board. Leukoreduction did not affect results. Murine RBCs were obtained from wild-type or hCD59 transgenic

C57BL/6J mice (42), which were used in accordance with a protocol approved by the Columbia University Institutional Animal Care and Use Committee. THP-1 cells (ATCC TIB-202) were grown in RPMI 1640 plus GlutaMAX plus 25 mM HEPES (Invitrogen) supplemented with 10% fetal bovine serum and 10 μg/ml ciprofloxacin.

DRM isolation. Human RBC suspensions (20%), treated with or without 1 μg/ml VLY at 37°C for 0.5 h, were solubilized in 1% Triton X-100 at 4°C for 1 h. DRMs were isolated as described previously (43).

Hemolysis assays. Hemolysis assays were done in Dulbecco's phosphate-buffered saline (DPBS) (7). Recombinant PFTs were expressed and purified as previously described (7, 44, 45) and used at 1 HU unless specified otherwise. For pharmacological or Ab inhibition, RBCs were pretreated with inhibitors for 1 h at 37°C. rFasL or MAb 2R2 (Enzo Life Sciences) was added with PFTs. None of the inhibitors tested affected RBC binding by a green fluorescent protein (GFP) fusion protein of the VLY binding domain (see Fig. S6 in the supplemental material). Eryptosis was induced with 950 mM sucrose or 1 mM $CaCl_2$ at 37°C for 18 h. For glucose uptake, RBCs were incubated with 5 mM glucose for 18 h, and glucose was removed by centrifugation.

Immunoprecipitation. Human RBC suspensions (20%) in DPBS were treated with PFTs (0.5 HU), rFasL (1 μg/ml), or bacteria (*G. vaginalis* or *S. intermedius* at an optical density at 600 nm [OD_{600}] of 0.6) for 30 min at 37°C and sonicated, and phosphatase inhibitor cocktail set III (1:100; Millipore) was added. THP-1 cells were adjusted to a concentration of 5×10^7 cells/ml and sonicated. Sonicates from either cell type were precleared with 200 μl of control agarose resin (Pierce); 10 μg of anti-RIP1 MAb G322-2 (BD) or anti-caspase-8 MAb 12F5 (AG Scientific) was added and incubated overnight at 4°C. Protein G plus agarose (100 μl; Pierce) was

added for 2 h at room temperature. Precipitates were suspended in 50 μl 1× NuPAGE LDS sample buffer and boiled.

Anti-CDC antibody. The anti-CDC polyclonal antibody was raised against VLY in rabbits and was described previously (31). This antibody cross-reacts with other CDCs as shown in Fig. S4 in the supplemental material.

Fluorescence assays. Human RBC suspensions (0.5%) were incubated with sublytic doses (<0.2 HU) of PFTs at 37°C for 1 h. To detect ROS, 2,7-dichlorofluorescein diacetate (20 μM; DCFDA; Invitrogen) was added. To detect ceramide or AGEs, RBCs were labeled with 10 μg/ml of 15B4 anticeramide MAb or anti-AGE polyclonal antibody (PAb) (Ab-Cam) for 1 h and anti-mouse IgM or IgG fluorescein isothiocyanate (FITC) conjugates for 1 h at 37°C and washed. To measure DRMs, diphenylhexatriene (DPH; Invitrogen) was added to samples at 2 μg/ml. Fluorescence was measured in an Infinite M200 (Tecan) at excitation/emission wavelengths of 495 nm/525 nm for DCFDA, 490 nm/525 nm for FITC, and 360 nm/430 nm for DPH. Cholesterol was measured using the Amplex red cholesterol assay kit (Invitrogen).

Immunoblots. For dot/Western blot assays, the following Abs were used: anti-RIP1 (BD; G322-2), anti-RIP3 (Thermo Scientific), anti-FADD (Millipore), anti-caspase-8 (AG Scientific), anti-CD59 (Thermo Scientific), anti-flotillin-1 (Sigma), anti-GM1 (AbCam), anti-GT1b (Millipore), anti-Fas (Thermo Scientific), anti-FasL (Thermo Scientific), and antihemoglobin (Santa Cruz) at dilutions of 1:1,000. For p-RIP1, anti-phospho-Ser/Thr (Cell Signaling Technology) was used at 1:500.

Bacterial growth assays. G. vaginalis strain ATCC 49145 was inoculated in brain heart infusion (BHI) broth with 10% fetal bovine serum at 37°C and 5% CO_2 with or without 5% human RBCs and grown for 18 h. S. intermedius strain ATCC 27335 and S. pneumoniae strain R6 were inoculated in Trypticase soy (TS) broth at 37°C with or without 5% human RBCs and grown for 5 h. For FasL inhibition, 5 μg/ml of NOK-1 or an irrelevant mouse IgG was added to the medium 1 h before inoculation. For rFasL experiments, 1 μg/ml was added with inocula. Growth was assessed by quantitative culture.

Statistics. Data are presented as means ± standard deviations (SD) from 3 experiments analyzed by the indicated statistical tests (GraphPad Prism).

SUPPLEMENTAL MATERIAL

Supplemental material for this article may be found at http://mbio.asm.org/lookup/suppl/doi:10.1128/mBio.01251-14/-/DCSupplemental.

Figure S1, TIF file, 0.2 MB.
Figure S2, TIF file, 0.1 MB.
Figure S3, TIF file, 0.2 MB.
Figure S4, TIF file, 0.1 MB.
Figure S5, TIF file, 0.1 MB.
Figure S6, TIF file, 0.1 MB.

REFERENCES

1. **Hod EA, Arinsburg SA, Francis RO, Hendrickson JE, Zimring JC, Spitalnik SL.** 2010. Use of mouse models to study the mechanisms and consequences of RBC clearance. Vox Sang. **99**:99–111. http://dx.doi.org/10.1111/j.1423-0410.2010.01327.x.
2. **Alaarg A, Schiffelers RM, van Solinge WW, van Wijk R.** 2013. Red blood cell vesiculation in hereditary hemolytic anemia. Front. Physiol. **4**:365. http://dx.doi.org/10.3389/fphys.2013.00365.
3. **Ucar K.** 2002. Clinical presentation and management of hemolytic anemias. Oncology (Williston Park) **16**(9 Suppl 10):163–170.
4. **Lang E, Qadri SM, Lang F.** 2012. Killing me softly—suicidal erythrocyte death. Int. J. Biochem. Cell Biol. **44**:1236–1243. http://dx.doi.org/10.1016/j.biocel.2012.04.019.
5. **Los FC, Randis TM, Aroian RV, Ratner AJ.** 2013. Role of pore-forming toxins in bacterial infectious diseases. Microbiol. Mol. Biol. Rev. **77**:173–207. http://dx.doi.org/10.1128/MMBR.00052-12.
6. **Tweten RK.** 2005. Cholesterol-dependent cytolysins, a family of versatile pore-forming toxins. Infect. Immun. **73**:6199–6209. http://dx.doi.org/10.1128/IAI.73.10.6199-6209.2005.
7. **Gelber SE, Aguilar JL, Lewis KL, Ratner AJ.** 2008. Functional and phylogenetic characterization of vaginolysin, the human-specific cytolysin from Gardnerella vaginalis. J. Bacteriol. **190**:3896–3903. http://dx.doi.org/10.1128/JB.01965-07.
8. **Wickham SE, Hotze EM, Farrand AJ, Polekhina G, Nero TL, Tomlinson S, Parker MW, Tweten RK.** 2011. Mapping the intermedilysin-human CD59 receptor interface reveals a deep correspondence with the binding site on CD59 for complement binding proteins C8alpha and C9. J. Biol. Chem. **286**:20952–20962. http://dx.doi.org/10.1074/jbc.M111.237446.
9. **Gillespie SH, Balakrishnan I.** 2000. Pathogenesis of pneumococcal infection. J. Med. Microbiol. **49**:1057–1067.
10. **Tran MP, Caldwell-McMillan M, Khalife W, Young VB.** 2008. Streptococcus intermedius causing infective endocarditis and abscesses: a report of three cases and review of the literature. BMC Infect. Dis. **8**:154. http://dx.doi.org/10.1186/1471-2334-8-154.
11. **Schwebke JR, Muzny CA, Josey WE.** 2014. Role of Gardnerella vaginalis in the pathogenesis of bacterial vaginosis—a conceptual model. J. Infect. Dis. **210**:338–343. http://dx.doi.org/10.1093/infdis/jiu089.
12. **Johnson AP, Boustouller YL.** 1987. Extra-vaginal infection caused by Gardnerella vaginalis. Epidemiol. Infect. **98**:131–137. http://dx.doi.org/10.1017/S0950268800061835.
13. **Lagacé-Wiens PR, Ng B, Reimer A, Burdz T, Wiebe D, Bernard K.** 2008. Gardnerella vaginalis bacteremia in a previously healthy man: case report and characterization of the isolate. J. Clin. Microbiol. **46**:804–806. http://dx.doi.org/10.1128/JCM.01545-07.
14. **Vandenabeele P, Galluzzi L, Vanden Berghe T, Kroemer G.** 2010. Molecular mechanisms of necroptosis: an ordered cellular explosion. Nat. Rev. Mol. Cell Biol. **11**:700–714. http://dx.doi.org/10.1038/nrm2970.
15. **Suzuki KG.** 2012. Lipid rafts generate digital-like signal transduction in cell plasma membranes. Biotechnol. J. **7**:753–761. http://dx.doi.org/10.1002/biot.201100360.
16. **Reeves VL, Thomas CM, Smart EJ.** 2012. Lipid rafts, caveolae and GPI-linked proteins. Adv. Exp. Med. Biol. **729**:3–13. http://dx.doi.org/10.1007/978-1-4614-1222-9_1.
17. **Ehrenschwender M, Wajant H.** 2009. The role of FasL and Fas in health and disease. Adv. Exp. Med. Biol. **647**:64–93. http://dx.doi.org/10.1007/978-0-387-89520-8_5.
18. **Mandal D, Mazumder A, Das P, Kundu M, Basu J.** 2005. Fas-, caspase 8-, and caspase 3-dependent signaling regulates the activity of the aminophospholipid translocase and phosphatidylserine externalization in human erythrocytes. J. Biol. Chem. **280**:39460–39467. http://dx.doi.org/10.1074/jbc.M506928200.
19. **Holler N, Zaru R, Micheau O, Thome M, Attinger A, Valitutti S, Bodmer JL, Schneider P, Seed B, Tschopp J.** 2000. Fas triggers an alternative, caspase-8-independent cell death pathway using the kinase RIP as effector molecule. Nat. Immunol. **1**:489–495. http://dx.doi.org/10.1038/82732.
20. **Degterev A, Hitomi J, Germscheid M, Che'n IL, Korkina O, Teng X, Abbott D, Cuny GD, Yuan C, Wagner G, Hedrick SM, Gerber SA, Lugovskoy A, Yuan J.** 2008. Identification of RIP1 kinase as a specific cellular target of necrostatins. Nat. Chem. Biol. **4**:313–321. http://dx.doi.org/10.1038/nchembio.83.
21. **Cho YS, Challa S, Moquin D, Genga R, Ray TD, Guildford M, Chan FK.** 2009. Phosphorylation-driven assembly of the RIP1-RIP3 complex regulates programmed necrosis and virus-induced inflammation. Cell **137**:1112–1123. http://dx.doi.org/10.1016/j.cell.2009.05.037.
22. **He S, Wang L, Miao L, Wang T, Du F, Zhao L, Wang X.** 2009. Receptor interacting protein kinase-3 determines cellular necrotic response to TNF-alpha. Cell **137**:1100–1111. http://dx.doi.org/10.1016/j.cell.2009.05.021.
23. **Zhang DW, Shao J, Lin J, Zhang N, Lu BJ, Lin SC, Dong MQ, Han J.** 2009. RIP3, an energy metabolism regulator that switches TNF-induced cell death from apoptosis to necrosis. Science **325**:332–336. http://dx.doi.org/10.1126/science.1172308.
24. **Sun L, Wang H, Wang Z, He S, Chen S, Liao D, Wang L, Yan J, Liu W, Lei X, Wang X.** 2012. Mixed lineage kinase domain-like protein mediates necrosis signaling downstream of RIP3 kinase. Cell **148**:213–227. http://dx.doi.org/10.1016/j.cell.2011.11.031.
25. **Vandenabeele P, Declercq W, Van Herreweghe F, Vanden Berghe T.** 2010. The role of the kinases RIP1 and RIP3 in TNF-induced necrosis. Sci. Signal. **3**:re4. http://dx.doi.org/10.1126/scisignal.3115re4.
26. **Vercammen D, Beyaert R, Denecker G, Goossens V, Van Loo G, Declercq W, Grooten J, Fiers W, Vandenabeele P.** 1998. Inhibition of

caspases increases the sensitivity of L929 cells to necrosis mediated by tumor necrosis factor. J. Exp. Med. **187:**1477–1485. http://dx.doi.org/10.1084/jem.187.9.1477.

27. **Van Herreweghe F, Mao J, Chaplen FW, Grooten J, Gevaert K, Vandekerckhove J, Vancompernolle K.** 2002. Tumor necrosis factor-induced modulation of glyoxalase I activities through phosphorylation by PKA results in cell death and is accompanied by the formation of a specific methylglyoxal-derived AGE. Proc. Natl. Acad. Sci. U. S. A. **99:**949–954. http://dx.doi.org/10.1073/pnas.012432399.

28. **Bratosin D, Estaquier J, Petit F, Arnoult D, Quatannens B, Tissier JP, Slomianny C, Sartiaux C, Alonso C, Huart JJ, Montreuil J, Ameisen JC.** 2001. Programmed cell death in mature erythrocytes: a model for investigating death effector pathways operating in the absence of mitochondria. Cell Death Differ. **8:**1143–1156. http://dx.doi.org/10.1038/sj.cdd.4400946.

29. **Lang F, Lang KS, Wieder T, Myssina S, Birka C, Lang PA, Kaiser S, Kempe D, Duranton C, Huber SM.** 2003. Cation channels, cell volume and the death of an erythrocyte. Pflugers Arch. **447:**121–125. http://dx.doi.org/10.1007/s00424-003-1150-8.

30. **Gatidis S, Zelenak C, Fajol A, Lang E, Jilani K, Michael D, Qadri SM, Lang F.** 2011. p38 MAPK activation and function following osmotic shock of erythrocytes. Cell. Physiol. Biochem. **28:**1279–1286. http://dx.doi.org/10.1159/000335859.

31. **Randis TM, Kulkarni R, Aguilar JL, Ratner AJ.** 2009. Antibody-based detection and inhibition of vaginolysin, the *Gardnerella vaginalis* cytolysin. PLoS One **4:**e5207. http://dx.doi.org/10.1371/journal.pone.0005207.

32. **Strasser A, Jost PJ, Nagata S.** 2009. The many roles of Fas receptor signaling in the immune system. Immunity **30:**180–192. http://dx.doi.org/10.1016/j.immuni.2009.01.001.

33. **Dosreis GA, Borges VM, Zin WA.** 2004. The central role of Fas-ligand cell signaling in inflammatory lung diseases. J. Cell. Mol. Med. **8:**285–293. http://dx.doi.org/10.1111/j.1582-4934.2004.tb00318.x.

34. **Hehlgans T, Pfeffer K.** 2005. The intriguing biology of the tumour necrosis factor/tumour necrosis factor receptor superfamily: players, rules and the games. Immunology **115:**1–20. http://dx.doi.org/10.1111/j.1365-2567.2005.02143.x.

35. **Bratosin D, Tcacenco L, Sidoroff M, Cotoraci C, Slomianny C, Estaquier J, Montreuil J.** 2009. Active caspases-8 and -3 in circulating human erythrocytes purified on immobilized annexin-V: a cytometric demonstration. Cytometry A **75:**236–244. http://dx.doi.org/10.1002/cyto.a.20693.

36. **Kriebardis AG, Antonelou MH, Stamoulis KE, Economou-Petersen E, Margaritis LH, Papassideri IS.** 2007. Storage-dependent remodeling of the red blood cell membrane is associated with increased immunoglobulin G binding, lipid raft rearrangement, and caspase activation. Transfusion **47:**1212–1220. http://dx.doi.org/10.1111/j.1537-2995.2007.01254.x.

37. **Berg CP, Engels IH, Rothbart A, Lauber K, Renz A, Schlosser SF, Schulze-Osthoff K, Wesselborg S.** 2001. Human mature red blood cells express caspase-3 and caspase-8, but are devoid of mitochondrial regulators of apoptosis. Cell Death Differ. **8:**1197–1206. http://dx.doi.org/10.1038/sj.cdd.4400905.

38. **Lang KS, Myssina S, Brand V, Sandu C, Lang PA, Berchtold S, Huber SM, Lang F, Wieder T.** 2004. Involvement of ceramide in hyperosmotic shock-induced death of erythrocytes. Cell Death Differ. **11:**231–243. http://dx.doi.org/10.1038/sj.cdd.4401311.

39. **Sagan D, Jermnim N, Tangvarasittichai O.** 2010. CD95 is not functional in human erythrocytes. Int. J. Lab. Hematol. **32:**e244–e247. http://dx.doi.org/10.1111/j.1751-553X.2010.01245.x.

40. **Matute-Bello G, Liles WC, Frevert CW, Dhanireddy S, Ballman K, Wong V, Green RR, Song HY, Witcher DR, Jakubowski JA, Martin TR.** 2005. Blockade of the Fas/FasL system improves pneumococcal clearance from the lungs without preventing dissemination of bacteria to the spleen. J. Infect. Dis. **191:**596–606. http://dx.doi.org/10.1086/427261.

41. **Dockrell DH, Lee M, Lynch DH, Read RC.** 2001. Immune-mediated phagocytosis and killing of Streptococcus pneumoniae are associated with direct and bystander macrophage apoptosis. J. Infect. Dis. **184:**713–722. http://dx.doi.org/10.1086/323084.

42. **Cowan PJ, Shinkel TA, Witort EJ, Barlow H, Pearse MJ, d'Apice AJ.** 1996. Targeting gene expression to endothelial cells in transgenic mice using the human intercellular adhesion molecule 2 promoter. Transplantation **62:**155–160. http://dx.doi.org/10.1097/00007890-199607270-00002.

43. **LaRocca TJ, Pathak P, Chiantia S, Toledo A, Silvius JR, Benach JL, London E.** 2013. Proving lipid rafts exist: membrane domains in the prokaryote Borrelia burgdorferi have the same properties as eukaryotic lipid rafts. PLoS Pathog. **9:**e1003353. http://dx.doi.org/10.1371/journal.ppat.1003353.

44. **Ratner AJ, Hippe KR, Aguilar JL, Bender MH, Nelson AL, Weiser JN.** 2006. Epithelial cells are sensitive detectors of bacterial pore-forming toxins. J. Biol. Chem. **281:**12994–12998. http://dx.doi.org/10.1074/jbc.M511431200.

45. **Rampersaud R, Planet PJ, Randis TM, Kulkarni R, Aguilar JL, Lehrer RI, Ratner AJ.** 2011. Inerolysin, a cholesterol-dependent cytolysin produced by Lactobacillus iners. J. Bacteriol. **193:**1034–1041. http://dx.doi.org/10.1128/JB.00694-10.